Robotics and Computer–Integrated Manufacturing 46 (2017) 94–103

Contents lists available at ScienceDirect

Robotics and Computer–Integrated Manufacturing

journal homepage: www.elsevier.com/locate/rcim

Modeling and design optimization of a robot gripper mechanism

Alaa Hassan[a,*], Mouhammad Abomoharam[b]

[a] University of Lorraine, Equipe de Recherche sur les Processus Innovatifs (ERPI), Nancy, France
[b] Higher Institute for Applied Sciences and Technology (HIAST), Damascus, Syria

ARTICLE INFO

Keywords:
Robot modeling
Multicriteria design optimization
NSGA-II
Sensitivity analysis

ABSTRACT

Structure modeling and optimizing are important topics for the design and control of robots. In this paper, we propose a process for modeling robots and optimizing their structure. This process is illustrated via a case study of a robot gripper mechanism that has a closed-loop and a single degree of freedom (DOF) structure. Our aim is to conduct a detailed study of the gripper in order to provide an in-depth step-by-step demonstration of the design process and to illustrate the interactions among its steps. First, geometric model is established to find the relationship between the operational coordinates giving the location of the end-effector and the joint coordinates. Then, equivalent Jacobian matrix is derived to find the kinematic model; and the dynamic model is obtained using Lagrange formulation. Based on these models, a structural multi-objective optimization (MOO) problem is formalised in the static configuration of the gripper. The objective is to determine the optimum force extracted by the robot gripper on the surface of a grasped rigid object under geometrical and functional constraints. The optimization problem of the gripper design is solved using a non-dominated sorting genetic algorithm version II (NSGA-II). The Pareto-optimal solutions are investigated to establish some meaningful relationships between the objective functions and variable values. Finally, design sensitivity analysis is carried out to compute the sensitivity of objective functions with respect to design variables.

1. Introduction

Robot design is a very complex process involving great modeling and simulation efforts. It has suffered an important progress in the last decades and many approaches deal with this issue. Major steps in robot manipulator design are; kinematics design, dynamics design, thermal design, and stiffness design [1]. In particular, robot modeling and structural analysis are required in all industries. To address these requirements, a design process is proposed in this paper that combines both; robot modeling and geometrical optimization. The proposed process is a sub-process of the general robotics design process in which modeling and optimization activities play essential and complementary roles in the design. As an illustrative case study, we carry out a modeling and an optimal design of a planar single degree of freedom (DOF) mechanism that is used for robot hands or grippers. These kind of mechanisms is amply used because of its simplicity and it only needs one actuator to move it, so many robots use this kind of mechanisms as gripper. However, many researches deal with geometric, kinematic, and dynamic modeling of the robots using different techniques. Some others work on optimization methods for multicriteria robot design optimization. A survey of these research works is presented in the following paragraphs.

Modeling is essential for design specifications, simulation, and advanced control of robots. Different techniques of modeling are available for modeling robots, especially for parallel and closed-loop robots due to their complexity [2–5]. Ibrahim and Khalil presented kinematic and dynamic modeling of three degrees of freedom 3-RPS (revolute, prismatic, and spherical) parallel robot [6]. This robot is characterized by a coupling between the 6-DOF of the platform. After presenting a (6×3) kinematic Jacobian matrix, they developed a reduced (3×3) Jacobian matrix relating the linear velocity of the platform with respect to the three actuated joints. In another paper, Khalil and Guegan presented closed form solutions for the inverse and direct dynamic models of the Gough-Stewart parallel robot. The models are obtained in terms of the Cartesian dynamic model elements of the legs and of the Newton-Euler equation of the platform [7]. Andrzej et al. used forward and inverse kinematic problem as well as working space and strength analysis issues for the construction of 3-DOF tripod electro-pneumatic parallel manipulator [8]. Qin et al. proposed analytical modeling of a two-staged parallel mechanism composed by a rigid platform in a serial connection with a compliant platform [9]. Hassan and Abomoharam performed a study of a gripper that has two closed loop structure. After finding geometric and kinematic models, they determined the geometrical solution space and verified it via a CAD

* Corresponding author: Postal address: 8 rue Bastien Lepage, 54000 Nancy, France.
E-mail address: alaa.hassan@univ-lorraine.fr (A. Hassan).

http://dx.doi.org/10.1016/j.rcim.2016.12.012
Received 26 July 2016; Received in revised form 26 December 2016; Accepted 27 December 2016
Available online 26 January 2017

model of the gripper [10]. Ha et al. employed Hamilton's principle, Lagrange multiplier, geometric constraints, and partitioning method to derive the dynamic equations of a slider-crank mechanism. They showed that dynamic formulation could give a good interpretation of a slider-crank mechanism by comparing the numerical simulations with experimental results [11]. Özgür and Mezouar exploited screw theory expressed via unit dual quaternion representation and its algebra to formulate both the forward (position and velocity) kinematics and pose control of an n-DOF robot arm [12].

Different researches of the optimum design of robot manipulators are available in the works of [13–16]. Xie et al. proposed a decoupled 3-DOF parallel tool head without parasitic motion. Using the atlases of the tool architecture as bases, the optimal kinematic design of the tool head is carried out [17]. Jiang et al. presented a dynamic modeling and redundant force optimization of a 2-DOF parallel kinematic machine with kinematic redundancy in order to minimize the position errors of the manipulated platform [18]. Nevertheless, in real robot design problems, the number of design parameters can be very large, and their influence on the value to be optimized (the objective function) can be very complicated, having a strongly non-linear character. In these complex cases, stochastic optimization techniques including evolutionary algorithms such as genetic algorithms (GA) may offer solutions to the problem [19]. Coello et al. proposed GA-based multiobjective optimization hybrid technique to optimize the counterweight balancing of a robot arm [20]. Jamwal et al. used a modified genetic algorithm to optimize the kinematic design of a parallel ankle rehabilitation robot [21]. Osyczka and Krenich discussed some new methods for multicriteria design optimization using evolutionary algorithms. The main aims of these methods is to reduce the computing time and to facilitate the decision making process. Examples of a robot gripper mechanism and a clutch break design are presented in this paper showing that these methods can be used to solve different design optimization problems [22]. Gao et al. described the implementation of genetic algorithms and artificial neural networks as an intelligent optimization tool for the dimensional synthesis of the spatial 6-DOF parallel manipulator. The multi-objective optimization (MOO) problem was consisted of two functions: system stiffness and dexterity, which are derived according to kinematic analysis of the parallel mechanism [23].

The rest of the paper is organized as follows. The proposed modeling and optimal design process of the robots and its advantages are described in Section 2. In Section 3, our case study of a robot gripper mechanism is described and its geometric modeling is recalled. Section 4 reviews the kinematic modeling of the gripper, then, the dynamic model is derived in Section 5. After describing and modeling the gripper, the corresponding multi-objective optimization problem is formalized in Section 6. Section 7 describes the solution algorithm of the optimization problem, and the non-dominated sorting genetic algorithm version II (NSGA-II), it discusses the results. Section 8 presents the sensitivity analysis of the gripper mechanism design. Finally, Section 9 summarizes the contributions and results made in this paper and gives some perspectives.

2. Modeling and optimal design process

The design of robots is a complex engineering task, in which certain mathematical models are required. This task can often be seen as an optimization problem in which the robot parameters or structure describing the best quality design is sought. In this paper, an integrated modeling-optimizing robot design process is proposed where the modeling steps are combined with the optimal structural design

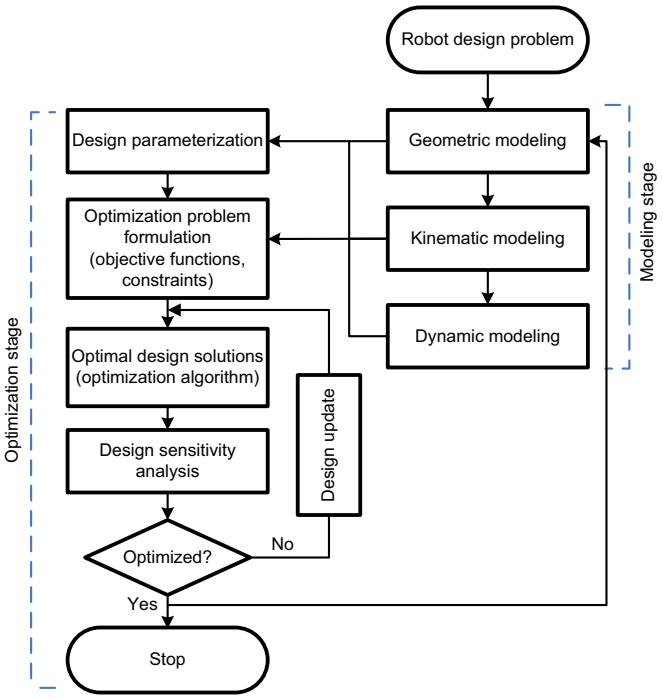

Fig. 1. Robot modeling and optimal design process.

process, Fig. 1 illustrates this proposed process. During this procedure, the geometric information is transferred from one step to the next step. The modeling stage information is captured as input by the optimization stage, while the optimal design information feeds back the modeling stage. These interactions give the designer the advantage to better define the design parameters and to take into account both the modeling and the optimization issues in one integrated process. These two issues are often handled separately as presented in the literature survey above, but in our presented process, they are combined together in order to benefit of their complementarity.

The process starts by defining the problem that must be solved. Depending on the objectives of the study, the applied steps may vary; it could be finding the geometric, kinetic, or dynamic models of the robot using different techniques. These models are important to apply high performance control algorithms, to improve stiffness, to increase payload, to improve force/torque capacity, etc. The objective could be also finding the optimal design that aims at enhancing the performance indexes by adjusting the structural parameters, such as the geometrical lengths. In the optimal design, several performance indices are involved, such as stiffness, transmission ratio, and accuracy.

The modeling stage starts by the geometric modeling, which represents the relations between the location vector of the end-effector X and the joint coordinate vector q (Eq. (1)). Several methods and notations have been proposed to find the geometric model; the most widely used one is that of Denavit-Hartenberg [24]. However, this method is developed for simple serial-structured robot. Khalil and Kleinfinger have proposed a unified description of parallel and tree-structured robots [25].

$$X=f(q) \tag{1}$$

Kinematic model is to find the relation between the end-effector velocity and the joint velocities. Kinematic model could be written using the Jacobian matrix J. This matrix appears in calculating the derivation of the geometric model. It gives the differential variations of the operational coordinates $\dot{X}$ in terms of the differential variations of the joint coordinates $\dot{q}$ (Eq. (2)). For parallel manip-

ulator, the key concept is to "break" the parallel manipulator into "simple" serial chains. Derived from the loop-closure or constraint equations, the equivalent Jacobian matrix could be found in terms of active and passive joint variables.

$$\dot{X}=J(q).\ \dot{q} \tag{2}$$

The Jacobian matrix has multiple applications in robotics. It facilitates the calculation of singularities and of the dimension of accessible operational space of the robot [26]. In static force model, we use the Jacobian matrix in order to calculate the forces and torques of the actuators in terms of the forces and moments exerted on the environment by the end-effector. The static model is essential in structural analysis as well as in formulating the optimal design problem.

The dynamic model is the relation between the torques (and/or forces) applied to the actuators and the joint positions, velocities and accelerations. The relation in Eq. (3) represents the dynamic model.

$$\Gamma=f(q,\ \dot{q},\ \ddot{q},\ \tau_{ext}) \tag{3}$$

where Γ is the joint torques and forces. q, $\dot{q}$, $\ddot{q}$ are the vectors of joint positions, velocities, and accelerations, respectively. τ_{ext} is the vector representing the external forces and moments that the robot exerts on its environment. The dynamic model is typically used in actuator dimensioning and in robot simulation and control. Several formalisms are used to obtain the dynamic model; the Lagrange multipliers, the principle of virtual work, and the Newton-Euler formulation.

The optimization stage is a process consists of design parameterization, optimization problem formulation, optimal design solutions, and design sensitivity analysis. The principal role of design parameterization is to define the geometric parameters that characterize the structural model of the robot and to collect a subset of the geometric parameters as design variables. Modeling stage supports design parameterization task by generating mathematical models that describe geometric structure, kinetic, and dynamic behaviours of the robot. Hence, geometric parameters and the structural design problem can be derived from the modeling stage. Only proper design parameterization will yield a good optimum design, since the optimization algorithm will search within a design space that is defined for the optimal design problem.

In optimization problem formulization step, stiffness, transmission ration, accuracy, cost, etc. can be defined by as objective functions with appropriate constraint bounds. This involves the selection of objective functions, expressed in terms of the design variables, which we seek to minimize or maximize. Beside the objective functions, it involves the selection of a set of variables to describe the design alternatives. Constraint functions are the criteria that the robot variables have to satisfy for each feasible design. In real world, it is common that a given structural design problem has multiple and often conflicting objectives. This will result in a multi-objective optimization problem from this step.

After defining the multi-objective design optimization problem, the next step is to find the optimal design solutions. The presence of multiple objectives in a problem, in principle, gives rise to a set of optimal solutions (largely known as Pareto-optimal solutions), instead of a single optimal solution. In the absence of any further information, one of these Pareto-optimal solutions cannot be said to be better than the other. This demands a user to find as many Pareto-optimal solutions as possible. Since evolutionary algorithms (EAs) work with a population of solutions, a simple EA can be extended to maintain a diverse set of solutions. With an emphasis for moving toward the true Pareto-optimal region, an EA can be used to find multiple Pareto-optimal solutions in one single simulation run. The NSGA-II proposed by Deb et al. [27], is one of the EAs widely used to solve MOO problems.

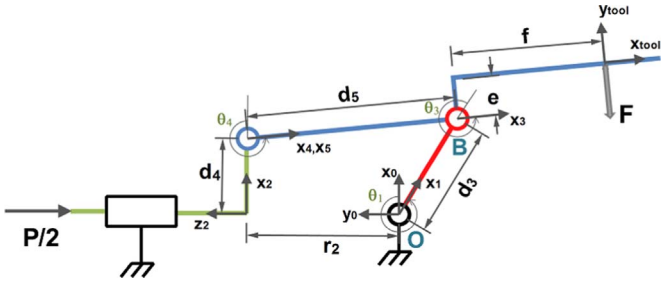

Fig. 2. Link frames of gripper mechanism.

Design sensitivity analysis is used to compute the sensitivity of objective functions with respect to design variables. Based on the design sensitivity results, a design engineer can decide on the direction and amount of design change needed to improve the objective functions. In addition, design sensitivity information can provide answers to "what if" questions by predicting objective function perturbations when the perturbations of design variables are provided. Regarding the geometric robot design, sensitivity analysis is of a great value to designers if a realistic and economical allocation of tolerances on design variables is to be achieved. There are different approaches to performing a sensitivity analysis like scatter plots, regression analysis, and partial derivative methods. Depending on the design problem, the design engineer could test some of the optimal solutions to improve the robot design at each iterative step. As a result, new designs could be obtained from optimization and sensitivity analysis steps. Thus, the geometric model, in the modeling stage, has to be updated for the optimal set of design variables supplied by the optimization stage.

In the rest of this paper, the proposed modeling and optimal design process is applied to a robot gripper mechanism. The motivation of this case study is to model this closed-loop structure, and then to design it optimally.

3. Description of the gripper mechanism and geometric modeling

The gripper is planner closed-loop mechanism with a single DOF. The gripping force F, applied on the object, is generated by the actuating force P. Due to the symmetry; we can perform the study on a half of the mechanism that is composed of three links and four joints (one prismatic and three revolute joints), as shown in Fig. 2.

The notations of Khalil and Kleinfinger [25], are used to describe the geometry of the closed-loop structure of the gripper. The definition of the local link frames are given in Fig. 2, while the geometric parameters are given in Table 1.

$P(j)$ denotes the frame antecedent to frame j, and σ_j =1 if joint j is prismatic and σ_j =0 if it is revolute. The homogeneous transformation matrix ${}^{i}T_j$, which defines the frame R_j relative to frame R_i, is obtained as a function of four geometric parameters (α_j, d_j, θ_j, r_j). Thus ${}^{i}T_j$, are obtained as:

Table 1
Geometric parameters of the gripper.

r_j	θ_j	d_j	α_j	σ_j	$P(j)$	j
0	θ_1	0	0	0	0	1
r_2	0	0	-90°	1	0	2
0	θ_3	d_3	0	0	1	3
0	θ_4	d_4	90°	0	2	4
0	0	$-d_5$	0	0	3	5

$$
{}^0T_1=\begin{bmatrix}\cos\theta_1 & -\sin\theta_1 & 0 & 0\\ \sin\theta_1 & \cos\theta_1 & 0 & 0\\ 0 & 0 & 1 & 0\\ 0 & 0 & 0 & 1\end{bmatrix},
$$

$$
{}^1T_3=\begin{bmatrix}\cos\theta_3 & -\sin\theta_3 & 0 & d_3\\ \sin\theta_3 & \cos\theta_3 & 0 & 0\\ 0 & 0 & 1 & 0\\ 0 & 0 & 0 & 1\end{bmatrix},
$$

$$
{}^3T_5=\begin{bmatrix}1 & 0 & 0 & -d_5\\ 0 & 1 & 0 & 0\\ 0 & 0 & 1 & 0\\ 0 & 0 & 0 & 1\end{bmatrix}
$$

$$
{}^3T_{tool}=\begin{bmatrix}1 & 0 & 0 & f\\ 0 & 0 & 1 & e\\ 0 & 0 & 1 & 0\\ 0 & 0 & 0 & 1\end{bmatrix},\quad {}^0T_2=\begin{bmatrix}1 & 0 & 0 & 0\\ 0 & 0 & 1 & r_2\\ 0 & -1 & 0 & 0\\ 0 & 0 & 0 & 1\end{bmatrix},
$$

$$
{}^2T_4=\begin{bmatrix}\cos\theta_4 & -\sin\theta_4 & 0 & d_4\\ 0 & 0 & -1 & 0\\ \sin\theta_4 & \cos\theta_4 & 0 & 0\\ 0 & 0 & 0 & 1\end{bmatrix} \tag{4}
$$

The geometric closed-loop constraint can be expressed as

$$
{}^0T_1{}^1T_3{}^3T_5={}^0T_2{}^2T_4 \tag{5}
$$

Thus

$$
\begin{aligned}&\theta_4=\theta_1+\theta_3\\ &d_3\cos\theta_1-d_5cos(\theta_1+\theta_3)=d_4\\ &d_3\sin\theta_1-d_5\sin(\theta_1+\theta_3)=r_2\end{aligned} \tag{6}
$$

4. Kinematic modeling

Let $\eta(q_1,\ldots,q_n)=\eta(\theta,\phi)=0$ be the constraint equations (Eq. (6)) previously found. Taking the time derivative and rearranging these Eq., Eq. 7 can be obtained as

$$
K(q)\dot{\theta}+K^*(q)\dot{\phi}=0 \tag{7}
$$

where $\theta=r_2$ is the actuated variable (joint) and $\phi=(\theta_1,\theta_3,\theta_4)^T$ are the passive variables (joints). n is the total number of the gripper joints, and m be the number of the actuated joints. Columns of the $((n-m)\times m)$ matrix $[K(q)]$ are the partial derivatives of $\eta(q)$ with respect to the actuated variables θ_i, i=1,..., m. Columns of the $((n-m)\times(n-m))$ matrix $[K^*(q)]$ are the partial derivatives of $\eta(q)$ with respect to the passive variables ϕ_i, i=1,..., n-m.

If $\det(K^*(q))\neq 0$, we can determine the linear and angular velocities of the passive joints ($\dot{\phi}$) in terms of only $\dot{\theta}$ (the linear and angular velocities of the actuated joints)

$$
\dot{\phi}=-(K^*)^{-1}K\,\dot{\theta} \tag{8}
$$

Hence, one can write the linear and angular velocities of the end-effector, denoted by tool in Fig. 2, with respect to the fixed coordinate frame R_O as

$$
\begin{aligned}&{}^0v_{tool}=J_v\,\dot{\theta}+J_v^*\,\dot{\phi}\\ &{}^0\omega_{tool}=J_\omega\,\dot{\theta}+J_\omega^*\,\dot{\phi}\end{aligned} \tag{9}
$$

which leads to

$$
\begin{aligned}&{}^0v_{tool}=\underbrace{(J_v-J_v^*(K^*)^{-1}K)}_{J_{v,eq}}\dot{\theta}\\ &{}^0\omega_{tool}=\underbrace{(J_\omega-J_\omega^*(K^*)^{-1}K)}_{J_{\omega,eq}}\dot{\theta}\end{aligned} \tag{10}
$$

Define the equivalent Jacobian matrix J_{eq} as

$$
J_{eq}=\begin{bmatrix}J_{v,eq}\\ J_{\omega,eq}\end{bmatrix} \tag{11}
$$

Eq. (9) can be written as

$$
V_{tool}\triangleq\begin{bmatrix}{}^0v_{tool}\\ {}^0\omega_{tool}\end{bmatrix}=J_{eq}\,\dot{\theta} \tag{12}
$$

Thus, kinematic model of the gripper can be found by the calculation of J_{eq}. The derivative of constraint equations Eq. (6) with respect to time gives

$$
K=\begin{bmatrix}0\\ 1\\ 0\end{bmatrix},
$$

$$
K^*=\begin{bmatrix}d_3\sin(\theta_1)-d_5\sin(\theta_1+\theta_3) & -d_5\sin(\theta_1+\theta_3) & 0\\ -d_3\cos(\theta_1)+d_5\cos(\theta_1+\theta_3) & d_5\cos(\theta_1+\theta_3) & 0\\ 1 & 1 & -1\end{bmatrix} \tag{13}
$$

The transformation matrix ${}^0T_{tool}={}^0T_1.\,{}^1T_3.\,{}^3T_{tool}$ is combined of rotation matrix ${}^0R_{tool}$ and translation vector ${}^0P_{tool}$ with respect to R_O

$$
\begin{aligned}{}^0T_{tool}&=\begin{bmatrix}\cos(\theta_1+\theta_3) & -\sin(\theta_1+\theta_3) & 0 & d3\cos(\theta_1)+f\cos(\theta_1+\theta_3)\\ & & & -e\sin(\theta_1+\theta_3)\\ \sin(\theta_1+\theta_3) & \cos(\theta_1+\theta_3) & 0 & e\cos(\theta_1+\theta_3)+d3\sin(\theta_1)\\ & & & +f\sin(\theta_1+\theta_3)\\ 0 & 0 & 1 & 0\\ 0 & 0 & 0 & 1\end{bmatrix}\\ &=\begin{bmatrix}{}^0R_{tool} & {}^0P_{tool}\\ 0\;0\;0 & 1\end{bmatrix}\end{aligned} \tag{14}
$$

The linear velocity of the tool ${}^0v_{tool}$ is calculated by the derivation of position vector ${}^0P_{tool}$ with respect to time

$$
\begin{aligned}{}^0v_{tool}=&\underbrace{\begin{bmatrix}0\\ 0\\ 0\end{bmatrix}}_{J_v}\dot{r}_2\\ &+\underbrace{\begin{bmatrix}-d_3\sin(\theta_1)-e\cos(\theta_1+\theta_3) & -e\cos(\theta_1+\theta_3)-f & 0\\ -f\sin(\theta_1+\theta_3) & \sin(\theta_1+\theta_3) & \\ d_3\cos(\theta_1)+f\cos(\theta_1+\theta_3) & f\cos(\theta_1+\theta_3)-e\sin & 0\\ -e\sin(\theta_1+\theta_3) & (\theta_1+\theta_3) & \\ 0 & 0 & 0\end{bmatrix}}_{J_v^*}\begin{bmatrix}\dot{\theta}_1\\ \dot{\theta}_3\\ \dot{\theta}_4\end{bmatrix}\end{aligned} \tag{15}
$$

While the angular velocity vector of the tool ${}^0\omega_{tool}$ is obtained from the angular velocity matrix Ω

$$
\Omega={}^0\dot{R}_{\text{tool}}.\,[{}^0R_{\text{tool}}]^T=\begin{bmatrix}0 & -\omega_z & \omega_y\\ \omega_z & 0 & -\omega_x\\ -\omega_y & \omega_x & 0\end{bmatrix},\quad {}^0\omega_{tool}=\begin{bmatrix}\omega_x\\ \omega_y\\ \omega_z\end{bmatrix} \tag{16}
$$

hence

$$
{}^0\omega_{tool}=\underbrace{\begin{bmatrix}0\\ 0\\ 0\end{bmatrix}}_{J_\omega}\dot{r}_2+\underbrace{\begin{bmatrix}0 & 0 & 0\\ 0 & 0 & 0\\ 1 & 1 & 0\end{bmatrix}}_{J_\omega^*}\begin{bmatrix}\dot{\theta}_1\\ \dot{\theta}_3\\ \dot{\theta}_4\end{bmatrix} \tag{17}
$$

Substituting Eqs. (13), (15), and (17) into Eq. (10) gives $J_{v,eq}$ and $J_{\omega,eq}$, then, the equivalent Jacobian matrix J_{eq} is obtained

$$J_{eq} = \begin{bmatrix} -\frac{\sin(\theta_1)(e\ \cos(\theta_1+\theta_3)+(d_5+f)\sin(\theta_1+\theta_3))}{d_5\sin(\theta_3)} \\ \frac{f\ \sin(\theta_1)(\cos(\theta_1+\theta_3))+(d_5\cos(\theta_1)-e\ \sin(\theta_1))\sin(\theta_1+\theta_3)}{d_5\sin(\theta_3)} \\ 0 \\ 0 \\ 0 \\ \frac{\sin(\theta_1)}{d_5\sin(\theta_3)} \end{bmatrix} \quad (18)$$

Based on the obtained kinematic model, we can establish the relationship between the external applied forces/torques and the joint forces/torques. To find this relationship, in our case study, the principle of virtual work is applied

$${}^0F_{tool}^T \cdot {}^0\delta X_{tool} = \tau^T \cdot \delta\theta \quad (19)$$

where ${}^0F_{tool}$ is the vector of the external forces/torques applied on the tool, assuming that there is no other external forces/torques. ${}^0\delta X_{tool}$ is the virtual displacement vector of the tool. τ is the vector of forces/torques applied on the actuated joints. $\delta\theta$ is the virtual displacement vector of the actuated joints.

Substituting Eq. (12) into Eq. (19) gives

$${}^0F_{tool}^T J_{eq}\ \delta\theta = \tau^T \cdot \delta\theta \quad (20)$$

Therefore

$$\tau = J_{eq}{}^T \cdot {}^0F_{tool} \quad (21)$$

Substituting

$${}^0F_{tool} = \begin{bmatrix} {}^0R_{tool}\begin{bmatrix} 0 \\ -F \\ 0 \end{bmatrix} \\ 0 \\ 0 \\ 0 \end{bmatrix} \quad (22)$$

$\tau = -P/2$, and J_{eq}(Eq. (18)) into Eq. (21), the relationship between the actuator force and the force applied on the object can be found

$$F = -\frac{d_5 P\ \sin(\theta_3)}{(d_5+2f)\sin(\theta_1)+d_5\sin(\theta_1+2\theta_3)} \quad (23)$$

Eq. (23) is resulted from kinematic modeling, and it will be transmitted to design parametrization. This relationship is the basis of the optimization problem formulization, as shown in the next paragraphs.

5. Dynamic modeling

To obtain dynamic model of the gripper, Lagrangian formulation is used. As above, n is the total number of joints, and m is the number of the actuated joints. The Lagrangian formulation for a closed-loop mechanism is

$$\frac{d}{dt}\left(\frac{\partial L}{\partial \dot{q}_i}\right) - \frac{\partial L}{\partial q_i} = Q_i + \sum_{j=1}^{n-m}\lambda_j\frac{\partial \eta_j}{\partial q_i} \quad , \quad i = 1, \ldots,n \quad (24)$$

where the scalar Lagrangian is defined from the total kinetic and potential energy

$$L(q,\dot{q}) = \sum_{i=1}^{n}(KE_i - PE_i) \quad (25)$$

KE_i kinetic energy of the link i.
PE_i potential energy of the link i.
Q_i the externally generalised forces applied on link i, it includes the actuator force/torque (if i is actuated) and the external forces/torques.
$q = [\theta_1\ \ \theta_3\ \ r_2]^T$ joint coordinate vector.
η_j $(n-m)$ loop-closure constraint equations.
λ_j $(n-m)$ Lagrange multipliers.

Eq. (24) can be written in matrix form

$$M(q)\ddot{q} + C(q,\dot{q})\dot{q} + G(q) = Q + \Psi^T\lambda \quad (26)$$

$M(q)$ $n \times n$ mass matrix.
$C(q,\dot{q})$ $n \times n$ Coriolis/centripetal matrix, where $C_{ij} = \frac{1}{2}\sum_{k=1}^{n}\left(\frac{\partial M_{ij}}{\partial q_k} + \frac{\partial M_{ik}}{\partial q_j} - \frac{\partial M_{kj}}{\partial q_i}\right)\dot{q}_k$
$G(q)$ $n \times 1$ vector of gravity terms, where $G_i = \frac{\partial(PE)}{\partial q_i}$
Ψ $(n-m) \times n$ constraint matrix that is obtained from the partial derivatives of $(n-m)$ constraint equations with respect to q_j, $\Psi_{ij} = \frac{\partial \eta_i}{\partial q_j}$

For the gripper mechanism, let (m_i, l_i, r_i, I_i), $i = 1, \ldots, n$, denote mass, length, center of gravity location, and component of inertia matrix of link i, respectively. For planar case, only $I_i = Iz_i$ is relevant, the gravity is along (-x_0) axis (Fig. 2). Thus, Eq. (26) matrices are written as

$$M(q) = \begin{bmatrix} m_1r_1^2 + Iz_1 + Iz_3 + m_3(l_1^2 - 2\cos(\theta_3)r_3l_1 + r_3^2) & Iz_3 + (r_3 - \cos(\theta_3)l_1)m_3r_3 & 0 \\ Iz_3 + (r_3 - \cos(\theta_3)l_1)m_3r_3 & m_3r_3^2 + Iz_3 & 0 \\ 0 & 0 & m_2 \end{bmatrix} \quad (27)$$

$$C(\dot{q},q) = \begin{bmatrix} \sin(\theta_2)l_1m_3r_3\dot{\theta}_2 & \sin(\theta_2)l_1m_3r_3(\dot{\theta}_1+\dot{\theta}_2) & 0 \\ -\sin(\theta_2)l_1m_3r_3\dot{\theta}_1 & 0 & 0 \\ 0 & 0 & 0 \end{bmatrix} \quad (28)$$

$$G(q) = \begin{bmatrix} g\ \sin(\theta_1+\theta_3)m_3r_3 - g\ \sin(\theta_1)(l_1m_3+m_1r_1) \\ g\ \sin(\theta_1+\theta_3)m_3r_3 \\ 0 \end{bmatrix} \quad (29)$$

$$\Psi(q) = \begin{bmatrix} \sin(\theta_1+\theta_3)d_5 - \sin(\theta_1)d_3 & \sin(\theta_1+\theta_3)d_5 & 0 \\ \cos(\theta_1)d_3 - \cos(\theta_1+\theta_3)d_5 & -\cos(\theta_1+\theta_3)d_5 & -1 \end{bmatrix} \quad (30)$$

Q $n \times 1$ vector of joint torque/force (τ) and externally applied torques/forces (τ_{ext}), this vector is written as

$$Q = \tau + \tau_{ext} \quad (31)$$

The actuating force vector is $\tau = [0\ \ -P/2\ \ 0]^T$ with respect to the fixed coordinate frame R_O.

The externally applied force is due to the gripping force F, and it is already expressed in Eq. (22). The externally applied force term in Lagrangian equation is

$$\tau_{ext} = \Im^T F \quad (32)$$

Where $\Im$ is the matrix of the relationship between the linear velocity of F application point ${}^0V_{tool}$ and the joint velocity $\dot{q} = [\dot{\theta}_1\ \ \dot{\theta}_3\ \ \dot{r}_2]^T$, i.e.

$${}^0V_{tool} = \Im \cdot \begin{bmatrix} \dot{\theta}_1 \\ \dot{\theta}_3 \\ \dot{r}_2 \end{bmatrix} \quad (33)$$

To find $\Im$, as in Eq. (15) and Eq. (17), we can obtain that

$${}^0V_{tool} = \underbrace{\begin{bmatrix} -d_3\sin(\theta_1) - e\cos(\theta_1+\theta_3) & -e\cos(\theta_1+\theta_3) - f & 0 \\ -f\ \sin(\theta_1+\theta_3) & \sin(\theta_1+\theta_3) & \\ d_3\cos(\theta_1) + f\ \cos(\theta_1+\theta_3) & f\ \cos(\theta_1+\theta_3) - e\ \sin & 0 \\ -e\ \sin(\theta_1+\theta_3) & (\theta_1+\theta_3) & \\ 0 & 0 & 0 \end{bmatrix}}_{\Im_v}\begin{bmatrix} \dot{\theta}_1 \\ \dot{\theta}_3 \\ \dot{r}_2 \end{bmatrix} \quad (34)$$

and

$${}^0\omega_{tool} = \underbrace{\begin{bmatrix} 0 & 0 & 0 \\ 0 & 0 & 0 \\ 1 & 1 & 0 \end{bmatrix}}_{\Im_\omega}\begin{bmatrix} \dot{\theta}_1 \\ \dot{\theta}_3 \\ \dot{r}_2 \end{bmatrix} \quad (35)$$

which leads to

$$\mathfrak{I} = \begin{bmatrix} \mathfrak{I}_v \\ \mathfrak{I}_\omega \end{bmatrix} = \begin{bmatrix} -e\cos(\theta_1+\theta_3) - d_3\sin(\theta_1) & -e\cos(\theta_1+\theta_3) - f & 0 \\ -f\sin(\theta_1+\theta_3) & \sin(\theta_1+\theta_3) & \\ d_3\cos(\theta_1) + f\cos(\theta_1+\theta_3) & f\cos(\theta_1+\theta_3) - e & 0 \\ -e\sin(\theta_1+\theta_3) & \sin(\theta_1+\theta_3) & \\ 0 & 0 & 0 \\ 0 & 0 & 0 \\ 0 & 0 & 0 \\ 1 & 1 & 0 \end{bmatrix} \tag{36}$$

Substituting the right side of Lagrangian equation Eq. (26) gives

$$Q + \Psi^T\lambda = \begin{bmatrix} fF + d_3(F\cos(\theta_3) - \sin(\theta_1)\lambda_1 + \cos(\theta_1)\lambda_2) \\ + d_5(\sin(\theta_1+\theta_3)\lambda_1 - \cos(\theta_1+\theta_3)\lambda_2) \\ fF + d_5(\sin(\theta_1+\theta_3)\lambda_1 - \cos(\theta_1+\theta_3)\lambda_2) \\ \frac{P}{2} - \lambda_2 \end{bmatrix} \tag{37}$$

After finding the dynamic model of the gripper, the relationship between the actuator force and the force applied on the object can be found. By setting the joint velocities, accelerations, and gravity terms to zero, we can find

$$\begin{bmatrix} 0 \\ 0 \\ 0 \end{bmatrix} = \begin{bmatrix} fF + d_3(F\cos(\theta_3) - \sin(\theta_1)\lambda_1 + \cos(\theta_1)\lambda_2) \\ + d_5(\sin(\theta_1+\theta_3)\lambda_1 - \cos(\theta_1+\theta_3)\lambda_2) \\ fF + d_5(\sin(\theta_1+\theta_3)\lambda_1 - \cos(\theta_1+\theta_3)\lambda_2) \\ \frac{P}{2} - \lambda_2 \end{bmatrix} \tag{38}$$

Solving this system of equations gives the relationship of the gripping force

$$F = -\frac{d_5 P\sin(\theta_3)}{(d_5+2f)\sin(\theta_1) + d_5\sin(\theta_1+2\theta_3)} \tag{39}$$

Eq. (39), which is resulted from the dynamic model, is the same one we found in Eq. (23) that is resulted from kinematic model. Depending on the study objectives, finding kinematic and/or dynamic model could be carried out, and both lead to the same static equation. This equation is transmitted to optimization stage, particularly to formulize the gripper optimization problem.

6. Optimization problem formulation

The goal of the optimization problem is to find the dimensions of the gripper elements and to optimize objective functions simultaneously by satisfying the geometric and force constraints. The vector of six design variables is $x = (d_3, d_4, d_5, l, e, f)$, where d_3, d_4, d_5, l, e, f are the gripper link variables used in geometrical modeling. The structure of geometrical dependencies of the mechanism is described in Fig. 3. The angles $\beta = \frac{\pi}{2} - \theta_1$ and $\alpha = \beta - \theta_3$ can be written in terms of the design variables as.

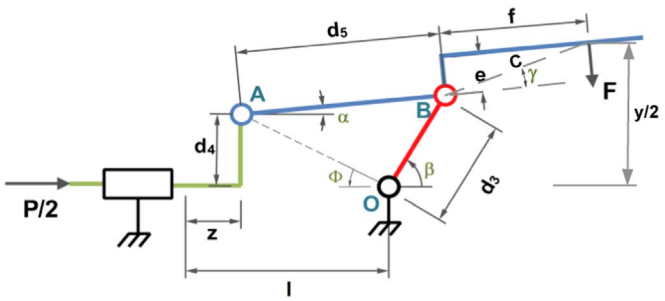

Fig. 3. Force distribution and geometrical variables of the gripper mechanism.

$$\alpha = \arccos\left(\frac{g^2 + d_5^2 - d_3^2}{2\,g\,d_5}\right) - \phi$$
$$\beta = \pi - \phi - \arccos\left(\frac{g^2 + d_3^2 - d_5^2}{2\,g\,d_3}\right) \tag{40}$$

where

$$g = \sqrt{d_4^2 + (l-z)^2}$$
$$\phi = \arctan\left(\frac{d_4}{l-z}\right)$$

6.1. Objective functions

Based on the relationship between the gripping force and the actuator force in Eq. (23) or Eq. (39), we can rewrite this relationship in terms of the design variables, α and β

$$F(x, z) = \frac{d_5\sin(\alpha-\beta)}{d_5\cos(\alpha)\cos(\alpha-\beta) + f\cos(\beta)}\,\frac{P}{2} \tag{41}$$

The objective functions of the gripper are borrowed from [22] to perform a bi-objective study to understand the trade-off between chosen objectives. These two objective functions can be formulated as follows:

1. The first objective function (Eq. (42)) can be written as the difference between the maximum and minimum gripping forces for the assumed range of gripper ends displacement. The minimization of this objective ensures that there is not much variation in the gripping force during the entire range of operation of the gripper. Thus, it ensures the minimization of stress variation in the gripper links.

$$f_1(x) = \max_z F(x, z) - \min_z F(x, z) \tag{42}$$

2. The second objective function (Eq. (43)) is the force transmission ratio, the ratio between the applied actuating force P and the resulting minimum gripping force at the tip of the gripper end. The minimization of this objective will ensure that the gripping force experienced at the tip of link f has the largest possible value. Thus, it ensure the maximization of force transmission ratio.

$$f_2(x) = \frac{P}{\min_z F(x, z)} \tag{43}$$

In the previously mentioned multi-objective optimization problem, both objective functions depend on the vector of decision variables and on the displacement z. The parameter z is the displacement parameter of the gripper actuator, which takes its minimum value at 0 and its maximum value at Z_{max}. Checking for a number of different solution vectors (x), it is observed that $Ff_1(x) = \max_z F(x, z) - \min_z F(x, z)$ is a decreasing function as shown in Fig. 4. So that, the maximum value of F takes place at $z = 0$ and the minimum value takes place at $z = Z_{max}$.

Thus, the objective functions may be written as:

$$f_1(x) = F(x, 0) - F(x, Z_{max})$$
$$f_2(x) = \frac{P}{F(x, Z_{max})} \tag{44}$$

6.2. Constraints

Before presenting the gripper constraints, we need to conclude the relationship between the displacement of the gripper end y and the displacement of the gripper actuator z (Fig. 3).

$$y(x, z) = 2(d_4 + d_5\sin(\alpha) + c\sin(\alpha+\gamma)) \tag{45}$$

where

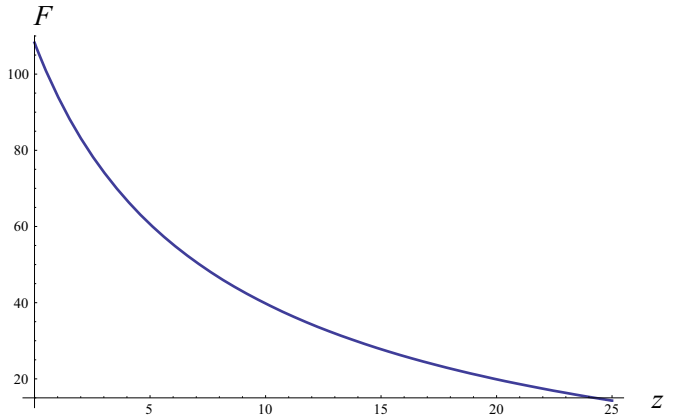

Fig. 4. Variation of force F with the displacement z for a typical design vector x.

$$c = \sqrt{f^2 + e^2}$$

$$\gamma = \arctan\left(\frac{e}{f}\right)$$

From the geometry of the gripper, a number of non-linear constraints can be derived:

1. The minimum displacement between the ends of gripper (corresponding to the maximum displacement of actuator value at Z_{max}) should be less than the minimum dimension of the gripping object

$$g_1(x) \;:\; Y_{min} - y(x, Z_{max}) > 0 \tag{46}$$

2. The distance between the gripper ends corresponding to Z_{max} should be greater than zero:

$$g_2(x) \;:\; y(x, Z_{max}) > 0 \tag{47}$$

3. The maximum distance between the gripping ends corresponding to no displacement of actuator ($z = 0$) should be greater than the maximum dimension of gripping object

$$g_3(x) \;:\; y(x, 0) - Y_{max} > 0 \tag{48}$$

4. Maximal range of the gripper ends displacement (Y_G) should be greater than or equal to the distance between the gripping ends corresponding to no displacement of actuator

$$g_4(x) \;:\; Y_G - y(x, 0) \geq 0 \tag{49}$$

5. Maximal displacement of actuator should be greater than l, the actuator stroke should not reach the point O(Fig. 3)

$$g_5(x) \;:\; l - Z_{max} > 0 \tag{50}$$

6. The gripper ends displacement (y) decreases when the actuator displacement (z) increases. To ensure this condition and to not reverse the gripper ends displacement direction, the angle β should be less than $\pi/2$:

$$g_6(x) \;:\; \beta(z = 0) < \frac{\pi}{2} \tag{51}$$

7. The angle α is the gripper declination refers to the horizontal axis, a stable gripping requires a limitation of this angle

$$g_7(x) \;:\; |\alpha| < 5^{\circ} \tag{52}$$

8. Geometrical properties are preserved by two constraints on α to maintain the triangle $\overset{\triangle}{OAB}$. From Eq. (40), the arccos function input should be less than 1

$$\left|\frac{g^2 + d_5^2 - d_3^2}{2\,g\,d_5}\right| < 1 \quad \Leftrightarrow \quad \left(\frac{g^2 + d_5^2 - d_3^2}{2\,g\,d_5}\right)^2 < 1$$

After simplification and substitution of g, we get:

$$\underbrace{(-(d_3 - d_5)^2 + d_4^2 + (l - z)^2)}_{a_1}\ \underbrace{((d_3 + d_5)^2 - d_4^2 - (l - z)^2)}_{a_2} > 0$$

So that, a_1 and a_2 should be positives for all $z \in [0, Z_{max}]$.

$$g_8(x) \;:\; d_4^2 + (l - Z_{max})^2 - (d_3 - d_4)^2 > 0 \tag{53}$$

$$g_9(x) \;:\; (d_3 + d_4)^2 - d_4^2 - l^2 > 0 \tag{54}$$

9. The geometric bounds of link lengths, or design variables, (in mm), are

$$10 \leq d_3 \leq 50$$
$$10 \leq d_4 \leq 50$$
$$10 \leq d_5 \leq 60$$
$$10 \leq l \leq 50$$
$$5 \leq e \leq 15$$
$$50 \leq f \leq 100$$

10. The geometric and force parameters are assumed to be as

$Y_{min} = 30$ mm ,

$Y_{max} = 70$ mm , $Y_G = 100$ mm, $Z_{max} = 25$ mm *and* $P = 95$ N

Thus, the gripper optimization problem can be formulated as follows:

Find $x^* = (d_3^*, d_4^*, d_5^*, l^*, e^*, f^*)$ which will satisfy the 9 inequality constraints

$$g_k(x) \quad k = 1, \ldots, 9 \tag{55}$$

and minimize the two objective functions

$$f(x^*) \;=\; \min\,[f_1(x), f_2(x)] \tag{56}$$

7. Solution algorithm and result discussion

After formulating the optimization problem, the next step is to find an optimal design solution using an appropriate algorithm. Our gripper case study is a MOO problem; and all of the above constraints must be taken into account. In order to solve it and find an optimal solution, there are several methods which are proposed in the literature. Due to the complexity, the size of problem and the importance of reducing the solving time, NSGA-II algorithm is used. This algorithm results in Pareto front that consists of a set of solutions, which are not dominated by each other. The Pareto-optimal solutions are thoroughly investigated to establish some meaningful relationships between the objective functions and variable values.

The NSGA-II procedure is illustrated in Fig. 5. In this procedure, an initial combined population (R_t) is randomly created and this population must be sort based on the non-domination strategy into each front. The fronts (F_1, F_2, F_3 ...) are compared with each other and a rank is assigned to each individual according to the fitness value. In addition, a new parameter, named crowding distance is calculated in order to sort the solutions of F_3. It is the distance of an individual to its neighbors, and the large value of this parameter shows the better diversity in population. The binary tournament selection is used to select the parents due to the rank and crowding distance. The mutation and crossover operators are utilized for the creation of a new offspring (Q_t

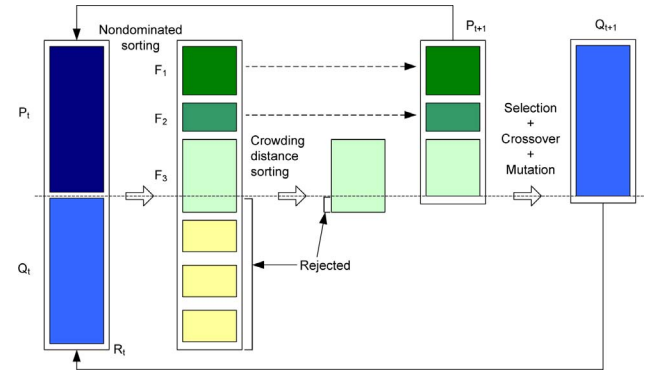

Fig. 5. NSGA-II procedure [28].

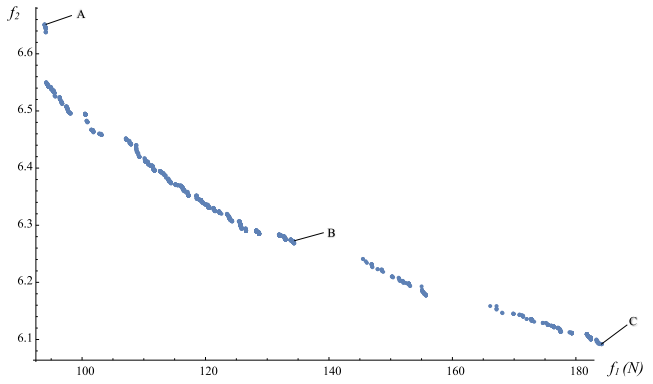

Fig. 6. Set of optimal solutions obtained using NSGA-II.

$_{+1}$) and so on for the next generations.

NSGA-II parameters are as follows: population size =200, number of generations =2000, probability of SBX (simulated binary crossover) recombination =0.9, probability of polynomial mutation =0.1, distribution index for real-variable SBX crossover =20, and distribution index for real-variable polynomial mutation =100.

Fig. 6 shows the obtained Pareto front resulting from NSGA-II optimization procedure. From this set of solutions, three are selected to investigate the changes in the gripper configuration. We have taken two extreme solutions (A and C) and one intermediate solution (B) as shown in Fig. 7. These three solutions are presented in Table 2, the design variable values are cited with their corresponding objective function values.

To investigate how one optimal solution varies from another, we can analyse the values of six design variables as a function of one of the objectives (the force transmission ratio for example). It is clear that variables e and f are fixed at their allowable lower limit value. We notice also that the force transmission ratio (f_2) is proportional to d_3, d_4, d_5, l design variables. On the other hand, the difference between the maximum and minimum gripping forces (f_1) is inversely proportional to these design variables. Therefore, the designer task is to select one of the optimal solutions compromising the two objective functions in terms of the design requirements.

8. Design sensitivity analysis

After selecting an optimal design solution, the last step is to analyse the design sensitivity to design variable changes. Design sensitivity analysis computes the rate of objective function change with respect to design variable changes. With the robot structural analysis, the design sensitivity analysis generates a critical information, gradient, for design optimization. Obviously, the objective function is presumed to be a differentiable function of the design, at least in the neighbourhood of the optimal solution point, which is found, and selected, in the previous step.

A sensitivity analysis of the mechanism is of a great value to designers if a realistic and economical allocation of tolerances on link-lengths is to be achieved. Such analysis enables the designer to notice important trends, to identify most critical link of a given mechanism, and to allocate the tolerances optimally [29]. In the gripper case study, the design variables are all link-lengths, so the attention is drawn to the effect of practical manufacturing tolerances on the objective functions. The local gripper design sensitivity to link-length tolerances is studied by using deterministic approach, based on the worst-case analysis of the individual tolerances (maximum output tolerance). Selecting an optimal solution (x^*) on point B, illustrated in Table 3, the gripper objective functions sensitivity can be conducted as follows.

Considering tolerances on link-lengths, the actual lengths of the links deviate from the nominal: $x_{i\,act} = x_{i\,nom} + \Delta x_i$. If the tolerances are much smaller than the link-lengths $t_i \ll x_i$, the variation in the objective function f_1 may be written in terms of Taylor series as:

$$\Delta f_1 = \Delta x^T.\ \nabla f_1(x^*) + \frac{1}{2}\Delta x^T.\ H_1(x^*).\ \Delta x \tag{57}$$

where

$$\Delta x = (\Delta d_3, \Delta d_4, \Delta d_5, \Delta l, \Delta e, \Delta f)$$

$\nabla f_1 = \frac{\partial f_1}{\partial x_i}$ is the first partial derivative of the objective function f_1 with respect to the ith design variable (x_i).
H_1 is the second partial derivative matrix called the Hessian matrix, $H_{1\,i,j} = \frac{\partial^2 f_1}{\partial x_i \partial x_j}$

In our case, the terms in Taylor series expansion having order three and above could be neglected without appreciable loss of accuracy. We also assume that the constraints are still satisfied when Δx_i occurs. The magnitude of the sensitivity coefficients for a design variable indicates the relative importance and influence of that variable on the variation of the objective function. Fig. 8 shows the values of the first order sensitivity coefficients of the objective function f_1 on the optimal solution point (x^*). It shows that the objective function f_1 is most sensitive to the variation of design variables d_5 and l, and less sensitive to the other variables.

The same formula in Eq. (57) is applied for the second objective function (f_2). Fig. 9 shows the values of the first order sensitivity coefficients of the objective function f_2 on the optimal solution point (x^*). Like f_1, the objective function f_2 is most sensitive to the variation of design variables d_5 and l. It is less (approximately equal) sensitive to the variables d_3 and d_4, and much less sensitive to e and f.

The variation of each objective function can now be evaluated when a rough manufacturing tolerances (variations) of the design variables are assigned, as illustrated in Table 4. The nominal values of the design variables are equal to the optimal solution values on point B, while the

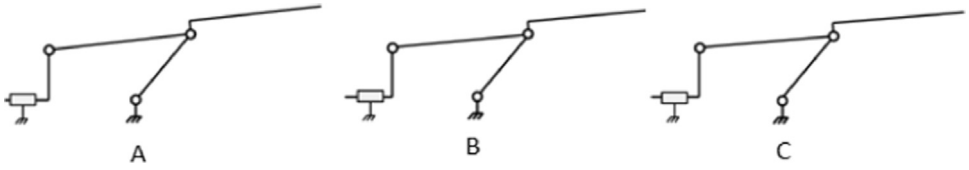

Fig. 7. Three gripper configurations for solutions A, B, and C.

Table 2
Objective function and design variable values for solutions A, B, and C.

Solution	f_1 (N)	f_2	d_3 (mm)	d_4 (mm)	d_5 (mm)	l (mm)	e (mm)	f (mm)
A	93.81	6.64	32.92	19.08	54.73	49.85	5.00	50.00
B	138.90	6.25	30.89	18.88	52.31	49.74	5.00	50.00
C	184.2	6.09	29.69	18.80	51.28	49.71	5.00	50.00

Table 3
Objective functions and selected optimal solution for point B.

Solution	f_1^* (N)	f_2^*	d_3^* (mm)	d_4^* (mm)	d_5^* (mm)	l^* (mm)	e^* (mm)	f^* (mm)
B	138.90	6.25	30.89	18.88	52.31	49.74	5.00	50.00

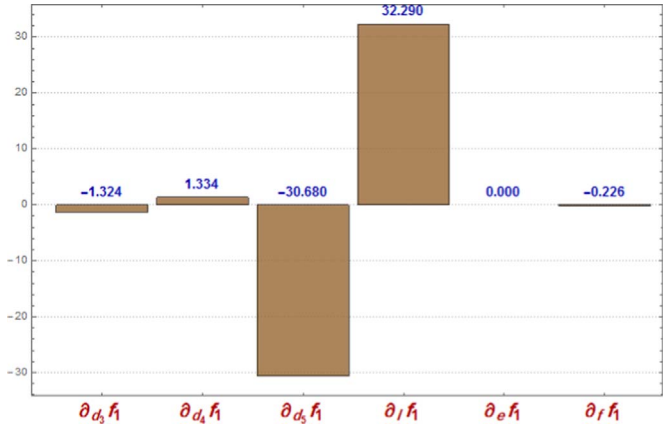

Fig. 8. First order sensitivity coefficients of f_1 to design variable variations on point B.

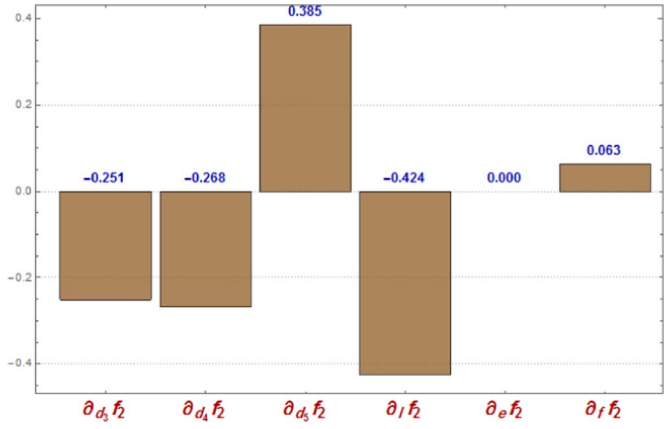

Fig. 9. First order sensitivity coefficients of f_2 to design variable variations on point B.

tolerances are derived from the International Tolerance Grades table in ISO 286. Based on the worst-case analysis, the total variation of an objective function is therefore the sum of the individual variations due to each of the design variables considered separately. From Eq. 57, the calculated maximum variation for each objective function is $\Delta f_1 = 22.4$ N, and $\Delta f_2 = 0.414$

Since d_5 and l have the major influences on the gripper objective functions, the tolerance intervals of these two variables can be restricted in order to get the objective function variations within acceptable limits. On the other hand, it is desirable to give as much of tolerance as possible to keep the manufacturing costs low. The designer has to select the optimal solution and the assigned tolerance

Table 4
Manufacturing tolerances (in mm) assigned to the gripper design variables.

Δd_3	Δd_4	Δd_5	Δl	Δe	Δf
±0.3	±0.2	±0.3	±0.3	±0.1	±0.3

intervals that compromise multiple conflicting design objectives. Once the optimal solution is selected, the geometric model must be updated and the optimization stage is completed.

9. Conclusion

This paper has proposed a two-stage process for modeling and optimizing robot structures. In the modeling stage, an analytical step-by-step study is introduced to find geometric, kinematic and dynamic models. The optimization stage shows the procedure to formulize and to solve a design optimization problem and then to analyse the design sensitivity. The data flow and interactions between these steps and stages are highlighted when a robot modeling and optimal design are needed. To illustrate the proposed process, a case study of a robot gripper is carried out. The process starts by the geometric modeling step to find the geometric closed-loop constraint equations of the gripper. Based on these equations, the kinematic model is derived in terms of equivalent Jacobian matrix and the velocity of the actuated joint, then, Lagrangian formulation is employed to find the dynamic model.

The modeling stage data is used in the optimization stage to formalize the optimization problem. The relationship between the gripper force and the actuator is resulting from the kinematic and dynamic models whereas some of geometrical constraints are derived from the geometrical model. Two objective functions are expressed: the minimization of the difference between the maximum and minimum gripping force and the maximization of the force transmission ratio. NSGA-II is applied to solve the problem resulting the Pareto-optimal solutions. Each one of these solutions represents a configuration of the gripper with a set the link variable values. A local sensitivity analysis of a trade-off solution has showed that the two objective functions are most sensitive to the variation of two design variables d_5 and l, and less sensitive to the other variables. The manufacturing tolerance intervals of these two variables can be restricted in order to maintain the objective function variations within acceptable limits.

Further improvements in this design process will focus on other MOO algorithms that may be used to find the optimal solutions. It is also vital to integrate multi-objective robust optimization principle in order to find multi-objectively robust Pareto optimum solutions.

References

[1] J. Ölvander, M. Tarkian, X. Feng, Multi-objective optimization of a family of industrial robots, in: L. Wang, A.H.C. Ng, K. Deb (Eds.), Multi-objective Evolutionary Optimisation for Product Design and Manufacturing., Springer, Netherlands, 2011, pp. 189–217.

[2] S. Bhattacharya, D.N. Nenchev, M. Uchiyama, A recursive formula for the inverse of the inertia matrix of a parallel manipulator, Mech. Mach. Theory 33 (7) (1998) 957–964.

[3] K. Miller, Optimal design and modeling of spatial parallel manipulators, Int. J. Robot. Res. 23 (2) (2004) 127–140.

[4] L.-W. Tsai, Solving the inverse dynamics of a Stewart-Gough manipulator by the principle of virtual work, J. Mech. Des. 122 (1) (2000) 3–9.

[5] M. Wang, M. Luo, T. Li, M. Ceccarelli, A unified dynamic control method for a redundant dual arm robot, J. Bionic Eng. 12 (2015) (361-37).

[6] O. Ibrahim, W. Khalil, Kinematic and dynamic modeling of the 3-RPS parallel manipulator, in: Proceedings of the 12th IFToMM World Congress, Besançon, France, 2007.

[7] W. Khalil, S. Guegan, Inverse and direct dynamic modeling of Gough-Stewart robots, IEEE Trans. Robot. Autom. 20 (4) (2004) 754–762.

[8] P.A. Laski, J.E. Takosoglu, S. Blasiak, Design of a 3-DOF tripod electro-pneumatic parallel manipulator, Robot. Auton. Syst. 72 (2015) 59–70.

[9] Y. Qin, K. Zhang, J. Li, J.S. Dai, Modelling and analysis of a rigid–compliant parallel mechanism, Robot. Comput.-Integr. Manuf. 29 (2013) 33–40.

[10] A. Hassan, Abomoharam. design of a single DOF gripper based on four-bar and slider-crank mechanism for educational purposes, Procedia CIRP 21 (2014) 379–384.

[11] J.-L. Ha, R.-F. Fung, K.-Y. Chen, S.-C. Hsien, Dynamic modeling and identification of a slider-crank mechanism, J. Sound Vib. 289 (2006) 1019–1044.

[12] E. Özgür, Y. Mezouar, Kinematic modeling and control of a robot arm using unit dual quaternions, Robot. Auton. Syst. 77 (2016) 66–73.

[13] D. Zhang, L. Wang, E. Esmailzadeh, PKM capabilities and applications exploration in a collaborative virtual environment, Robot. Comput.-Integr. Manuf. 22 (4) (2006) 384–395.

[14] P.R. Bergamaschi, A.C. Nogueira, F.P. Saramago, Design and optimization of 3R manipulators using the workspace features, Appl. Math. Comput. 172 (1) (2006) 439–463.

[15] B.K. Rout, R.K. Mittal, Parametric design optimization of 2-DOF R–R planar manipulator: a design of experiment approach, Robot. Comput.-Integr. Manuf. 24 (2) (2008) 239–248.

[16] A. Yu, I.A. Bonev, Z.M. Paul, Geometric approach to the accuracy analysis of a class of 3-DOF planar parallel robots, Mech. Mach. Theory 43 (3) (2008) 364–375.

[17] F. Xie, X.-J. Liu, J. Wang, A 3-DOF parallel manufacturing module and its kinematic optimization, Robot. Comput.-Integr. Manuf. 28 (2012) 334–343.

[18] Y. Jiang, T.-M. Li, L.-P. Wang, Dynamic modeling and redundant force optimization of a 2-DOF parallel kinematic machine with kinematic redundancy, Robot. Comput.-Integr. Manuf. 32 (2015) 1–10.

[19] G. Renner, A. Ekart, Genetic algorithms in computer aided design, Comput.-Aided Des. 35 (2003) 709–726.

[20] C. Coello, A. Christiansen, A. Aguirre, Using a new GA-based multiobjective optimization technique for the design of robot arms, Robotica 16 (1998) 401–414.

[21] P. Jamwal, S. Xie, K. Aw, Kinematic design optimization of a parallel ankle rehabilitation robot using modified genetic algorithm, Robot. Auton. Syst. 57 (2009) 1018–1027.

[22] A. Osyczka, S. Krenich, Some methods for multicriteria design optimization using evolutionary algorithms, J. Theor. Appl. Mech. 42 (3) (2004) 565–584.

[23] Z. Gao, D. Zhang, Y. Ge, Design optimization of a spatial six degree-of-freedom parallel manipulator based on artificial intelligence approaches, Robot. Comput.-Integr. Manuf. 26 (2010) 180–189.

[24] J. Denavait, R.S. Hartenberg, A kinematic notation for lower pair mechanism based on matrices, J. Appl. Mech. 22 (1955) 215–221.

[25] W. Khalil, J. Kleinfinger, A new geometric notation for open and closed-loop robots, in: Proceedings of the IEEE conference on robotics automation:1174–1180, 1986.

[26] P. Paul, Robot manipulators: mathematics, programming and control, MIT Press, Cambridge, 1981.

[27] K. Deb, S. Agrawal, A. Pratap, T. Meyarivan, A fast and elitist multi-objective genetic algorithm: NSGA-II, IEEE Trans. Evolut. Comput. 6 (2) (2002) 182–197.

[28] K. Deb, R.B. Agarwal, Simulated binary crossover for continuous search space, Complex Syst. 9 (1995) 115–148.

[29] N. Pavlović, Analysis of mechanical error in quick-return shaper mechanism, in: Proceedings of the 12th IFToMM World Congress, Besançon, France, 2007.